On the Kinetics of the Formation of Small Micelles. 1. Broadband Ultrasonic Absorption Spectrometry

T. Telgmann and U. Kaatze*

Drittes Physikalisches Institut, Georg-August-Universität, Bürgerstrasse 42-44, D-37073 Göttingen, Germany

Received: February 27, 1997; In Final Form: June 23, 1997[⊗]

At 25 °C the ultrasonic absorption spectra between 100 kHz and 2 GHz, the sound velocities, and the shear viscosities of aqueous solutions of *n*-heptylammonium chloride have been measured at the critical micelle concentration (cmc) and also at concentrations above the cmc. The term cmc denotes a concentration range rather than a well-defined value here. The absorption spectra reveal two relaxation regions, one at frequencies around a few megahertz and the other one at around 1 GHz. The low-frequency relaxation may be attributed to the exchange of surfactant monomers between the micelles and the suspending phase. In contrast to the theoretical predictions from the accepted models of the kinetics of micelle formation, however, the low-frequency process is subject to a relaxation time distribution. The width of the distribution function is particularly large near the cmc. Close to the cmc, in addition, the relaxation time and relaxation amplitude do not follow the theoretically predicted dependences upon concentration. In conformity with previous findings, the high-frequency relaxation seems to be partly due to the mechanism of chain isomerization in the micellar cores. However, estimations show that the process of rotational isomerization cannot fully account for the measured facts. It is assumed that, at least at solute concentrations in the cmc region and slightly above the cmc, a variety of geometrically less defined supramolecular structures exist in the solutions of amphiphiles rather than globular micelles that follow a comparatively narrow size distribution. This idea is supported by the shear viscosity data.

1. Introduction

Self-association of amphiphilic molecules to form micellar structures in water is a phenomenon of current wide interest, not just for fundamental aspects in condensed-matter physics but also for a variety of applications in biological processes and chemical engineering.[1,2] Being a complex multiple equilibrium process, however, the mechanism of micelle formation is still incompletely understood. It is now generally accepted that the self-association of amphiphiles is governed by their tendency to reduce the thermodynamically unfavorable effect of hydrophobic hydration around them.[3] It is also widely assumed that the kinetics of micelle formation can be basically represented by the model of Aniansson and Wall[4,5] who supposed the interactions between the micelles and the suspending phase can be expressed by a scheme of coupled chemical reactions

$$N_1 + N_{i-1} \underset{k_i^b}{\overset{k_i^f}{\rightleftharpoons}} N_i \qquad (1)$$

where $i = 2, 3, \ldots$ denotes the number of amphiphiles per multimer N_i. The quantities k_i^f and k_i^b are the forward and backward rate constants of reaction "*i*", respectively. Using the reaction scheme defined by eq 1, it is supposed that the concentration of monomers N_1 is always much higher than that of multimers so that reactions between aggregates do not have to be considered. In applications of the Aniansson−Wall approach, a direct contribution to the sonic spectrum from oligomers is excluded by the presumed shape of the size distribution in thermal equilibrium of *i*-mers (Figure 1). According to the size distribution displayed in Figure 1 there is in fact a large concentration of monomers, nearly equal to the critical micelle concentration (cmc), but there are almost no oligomers in the solution. The size distribution of micelles is assumed to be symmetrically bell shaped around the mean aggregation number $\bar{m}$.

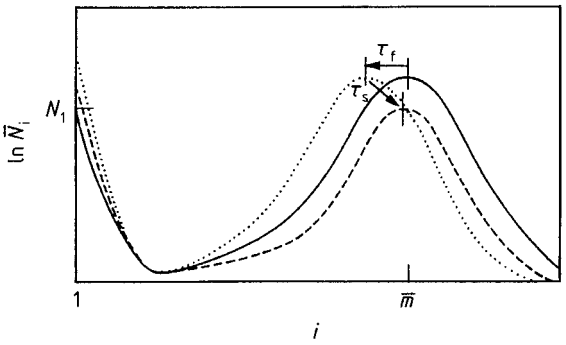

Figure 1. Distribution of the equilibrium concentration $\bar{N}_i$ of molecular aggregates made of *i* amphiphile monomers (full curve). $\bar{m}$ denotes the mean aggregation number at equilibrium. Dotted and dashed curves indicate the response of the system to a fast change in external parameters. The approach of the new equilibrium may be subdivided into two steps, one characterized by a fast (τ_f) the other one by a slower (τ_s) relaxation process.[13]

Because of the different states of hydration monomers dissolved in the suspending phase and incorporated in micelles, they exhibit different molar volumes and enthalpies. Chemical relaxation methods such as pressure jump and temperature jump techniques as well as sonic spectrometry[6] can thus be favorably used to study the kinetics of micelle formation and to verify the Aniansson−Wall theory. To derive relations suitable for such verification between parameters of the micelle solutions and parameters of ultrasonic spectra, Teubner and Kahlweit considered the Aniansson−Wall model assuming small disturbances from thermal equilibrium due to harmonically alternating sonic fields.[7,8] Two relaxation processes with discrete relaxation times were identified. These processes can be related in a suggestive manner to steps in the reformation of the equilibrium

[⊗] Abstract published in *Advance ACS Abstracts,* September 1, 1997.

S1089-5647(97)00747-5 CCC: $14.00 © 1997 American Chemical Society

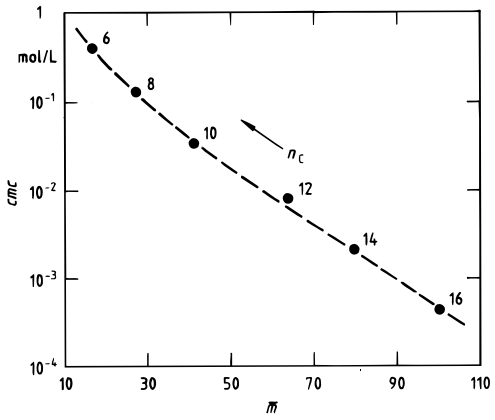

Figure 2. Critical micelle concentration cmc (as usually given in the literature) versus the mean aggregation number $\bar{m}$ for aqueous solutions of a series of sodium alkyl sulfates $CH_3(CH_2)_{n_C-1}SO_4Na$ at 25 °C.[14]

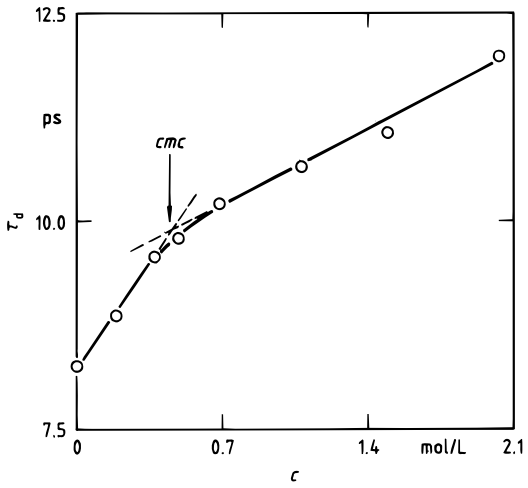

Figure 3. Principal dielectric relaxation time τ_d of aqueous solutions of C_7ACl at 25 °C displayed as a function of amphiphile concentration c.[15,16]

distribution as indicated by Figure 1. The size distribution of micelles first follows an external excitation by a fast exchange of monomers between micelles, characterized by a relaxation time τ_f on the order of microseconds. The number of micelles is not altered thereby. In parallel to this process, the new equilibrium between the micelles and the suspending liquid is adapted by monomer exchange between both phases with a considerably longer relaxation time τ_s on the order of milliseconds or even seconds. The latter process involves a change of the number density of micelles.

Broadband ultrasonic absorption studies of aqueous solutions of anionic, cationic, zwitterionic, and nonionic micelles, however, reveal more complicated spectra.[9,10] All micelle systems exhibit a relaxation term with relaxation time τ_h between about 0.1 and 0.3 ns (25 °C). In addition, process "f" appears not to be one Debye-type relaxation mechanism with discrete relaxation time.[9] Therefore, it is of great interest to reconsider the Aniansson−Wall and Teubner−Kahlweit models. We particularly focus on possible effects from neglecting interaggregate forces, which, on one hand, might lead to a modification of the reaction scheme (eq 1) to also include association of multimers. Interaggregate forces, on the other hand, could also result in fluctuating clusters of micelles, associated by characteristic sonic spectra as predicted, for example, by the Romanov−Solov'ev theory of noncritical concentration fluctuations.[11,12] It is an obvious assumption to expect the effects of multimer association, which have been neglected so far, to be particularly important in systems of small mean aggregation number $\bar{m}$ of micelles. Before analyzing the theoretical models of micelle formation, we therefore first measured in the frequency range from 100 kHz to 2 GHz ultrasonic absorption spectra of solutions of small micelles as a function of total concentration of amphiphiles. As ilustrated by Figure 2 small $\bar{m}$ values correspond with large values of the cmc. Hence we completed previous studies of cationic micelle solutions using n-heptylammonium chloride as surfactant with the high cmc of around 0.4 mol/L. The well-known term cmc is used though it denotes a concentration range of considerable width here (0.4 ... 0.6 mol/L, Figure 3). In the second part of this study[38] a treatment will thus be presented in which a well-defined cmc in the sense of a single concentration is not required.

2. Experimental Section

Surfactant Solutions. A 1 M solution of *n*-heptylammonium chloride ($CH_3(CH_2)_6NCl$, C_7ACl, molar weight 151.68 g/mol) has been prepared from the amine (Fluka, Neu-Ulm, FRG; >98%) by successively adding hydrochloride acid (Merck, Darmstadt, FRG; >99.9%). In doing so the hydrogen ion concentration was continuously measured with the aid of a pH-meter (Schott CG 707 with glass electrode H 65). Solutions of lower C_7ACl content have been obtained by adding appropriate amounts of water that had been deionized by mixed-bed ion exchange and distilled afterward. The density ρ of the solutions has been measured using a pycnometer that had been calibrated against degassed water. The shear viscosity η_s of the samples has been determined with the aid of a falling ball viscometer (Haake B/BH). A survey of the solutions measured in this study is given in Table 1 where some additional parameters are also presented. In Figure 3 the principal dielectric relaxation time τ_d of the water in aqueous C_7ACl solutions is displayed as a function of solute concentration to show that there exists a broad transition region in the concentration dependence of parameters rather than a sharp transition at a well-defined cmc, as mentioned before.

Ultrasonic Absorption Spectrometry. The sound absorption coefficient α of the sample liquids has been determined between 100 kHz and 2 GHz using two different frequency domain methods and altogether seven different specimen cells. Besides the contribution α_{exc} from sonic excess absorption in which we are interested here, the total absorption coefficient of the liquids contains also a "classical" part α_{cl} that according to[17]

$$\alpha_{cl}(\nu) = \nu^2 B/c_s(\nu) \qquad (2)$$

substantially increases with frequency ν. In eq 2 denotes B a parameter that is independent of ν, and $c_s(\nu)$ is the sound velocity of the sample. In view of the frequency dependence of α_{cl}, we applied a resonator method especially matched to the small sample loss at low frequencies (0.1 MHz $\leq \nu \leq$ 8 MHz) and a pulse-modulated traveling-wave method specially designed for the large α-values at high frequencies (3 MHz $\leq \nu \leq$ 2000 MHz). We used three biplanar circular cylindrically shaped resonator cells[18,19] differing from another by their diameter, cell length, and fundamental frequency ν_T of the longitudinal transducer vibrations (ν_T = 1 MHz:0.4−4 MHz; ν_T = 2 MHz:0.4−7 MHz; ν_T = 5 MHz:2.5−8 MHz). A plano-concave specimen cell,[20] particularly constructed to reduce diffraction losses at low frequencies, was used at frequencies between 0.1 and 2 MHz (ν_T = 1 MHz). Undesired higher-order spurious modes within the cavity resonator have been carefully taken into account. For this purpose the complex resonator transfer function has been always recorded in the

TABLE 1: Parameters of the Aqueous Solutions of *n*-Heptylammonium Chloride at 25 °C: Molar (c) and Molal (c^*) Concentration as Well as Mole Fraction x_m of Solute, Molar Concentration c_w of Water, Density ρ, Shear Viscosity η_s, and Sound Velocity c_s at Two Frequencies

c, mol/L, ±0.1%	c^*, mol/kg, ±0.1%	x_m, 10^{-2}, ±0.1%	c_w, mol/L, ±0.1%	ρ, g/cm^3, ±0.1%	η_s, 10^{-2}g/(cm s), ±2%	c_s(300 kHz), m/s, ±0.5%	c_s(520 MHz), m/s, ±1%
0.40	0.426	0.763	52.0	0.998	1.08	1553	1553
0.45	0.483	0.866	51.5	0.997	1.11	1558	1561
0.50	0.542	0.969	51.1	0.996	1.12	1560	1565
0.60	0.661	1.179	50.2	0.996	1.20	1560	1567
0.80	0.913	1.622	48.5	0.995	1.35	1558	1569
1.00	1.183	2.093	46.8	0.994	1.60	1557	1568

relevant frequency range around the resonance peak under consideration, using a computer-controlled network analyzer. The correct resonance frequency and quality factor of this peak have been obtained from fitting suitable analytical expressions to the measured complex transfer function data. Unavoidably present instrumental loss required calibration measurements in which the liquid under test was replaced by a reference liquid of well-known attenuation coefficient and with sound velocity and density as close as possible to the sample c_s and ρ. We used aqueous NaCl and methanol solutions as reference. At frequencies above 3 MHz absolute measurements of α have been performed applying a method in which a pulse-modulated traveling wave of frequency ν was transmitted through a cell of variable sample length. Possibly existing small instabilities and nonlinearities of the electronic apparatus were taken into account by a direct comparator technique in which the sample cell is substituted for a precisely adjustable reference attenuator.[21] We used three different specimen cells; two of them were operated at odd overtones of the fundamental frequency ν_T of their transducers (ν_T = 1 MHz:3−60 MHz;[22] ν_T = 10 MHz: 30−500 MHz[23]). The other cell had been constructed to utilize broadband surface excitation of small piezoelectric lithium niobate rods[24] according to the principle by Bömmel and Dransfeld.[25]

Sound Velocity Measurements. In the lower part of the frequency range of measurements the sound velocity c_s of the samples has been derived from the distances between a series of resonance frequencies of the cavity resonator cells using appropriate theoretical expressions.[19,20] At frequencies above 3 MHz, c_s has been determined from the standing wave pattern in the receiver signal versus cell length relation, resulting from multiple reflections within the transmission cells at small transducer spacing.[24]

Experimental Accuracy. Multiple data recording followed by averaging and digital filtering procedures and a suitable regression analysis lead to negligibly small statistical errors in both the α- and c_s-values. The measuring frequency ν was known and kept constant with an error that was also negligibly small. The temperature of the sample cells was controlled to within ±0.01 K. Temperature gradients within the cells and deviations in the temperature of different cells thus did not exceed 0.05 K, corresponding to an uncertainty of 0.15% in the α-values of the liquids. Together with errors that are specific for each particular apparatus, the following uncertainties result in the data of the absorption coefficient: $\Delta\alpha/\alpha = 0.06$, 0.1−3 MHz; $\Delta\alpha/\alpha = 0.025$, 3−30 MHz; $\Delta\alpha/\alpha = 0.01$, 30−500 MHz; $\Delta\alpha/\alpha = 0.015$, 500−2000 MHz. The errors in the sound velocity are somewhat smaller: $\Delta c_s/c_s = 0.005$, 0.1−500 MHz; $\Delta c_s/c_s = 0.01$, 500−2000 MHz. Due to the overlaps in the frequency range of different apparatus and cells, unnoticed errors exceeding these values appear to be most unlikely.

3. Results and Treatment of Data

Absorption Spectra of Micelle Solutions. In Figure 4 the measured ultrasonic spectra for two C_7ACl solutions are presented in a suggestive plot in which the excess attenuation per wavelength

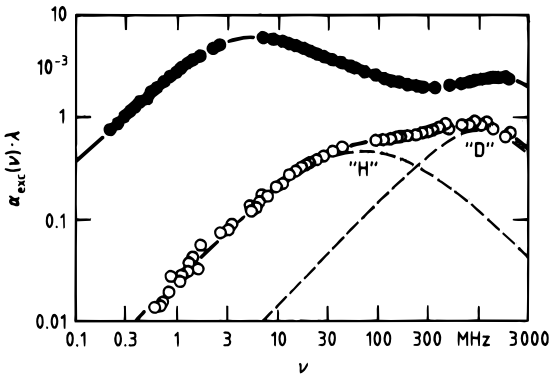

Figure 4. Sonic excess absorption spectra for two aqueous C_7ACl solutions at 25 °C: ○, 0.4 mol; ●, 0.5 mol/L. The dashed curves indicate the subdivision of the former spectrum into a Hill ("H") and a Debye ("D") relaxation term. The full curves represent the sum of such terms with the parameter values found in the fitting procedures (Tables 2, 3).

$$\alpha_{exc}(\nu)\lambda = \alpha(\nu)\lambda - \alpha_{cl}(\nu)\lambda = \alpha(\nu)\lambda - B\nu \qquad (3)$$

is displayed as a function of ν. Here $\lambda = c_s(\nu)/\nu$ denotes the wavelength of the sonic field within the liquid. The $\alpha_{exc}(\nu)\lambda$ spectrum of the 0.5 M solution clearly exhibits two relative maxima, indicating that there exist at least two absorption regions. The frequency of the maximum of the low-frequency absorption region, roughly 5 MHz, corresponds with the aforementioned relaxation time τ_f in the Aniansson−Wall and Teubner−Kahlweit theories of the micelle kinetics. The maximum of the other absorption term is found at a frequency around 1 GHz, in conformity with the previous findings for micelle systems[9,10] mentioned in the Introduction. With the 0.4 M C_7ACl solution the low-frequency absorption term obviously is substantially shifted toward higher frequencies. To extract from the measured spectra more details on the underlying absorption terms and on the dependence of their parameters on the surfactant concentration, we tried to represent the $\alpha\lambda$-data by relaxation spectral functions $R(\nu)$. For this purpose the measured data have been fitted to relevant analytical functions using a nonlinear least-squares regression analysis to minimize the variance

$$\chi^2 = \frac{1}{N-P-1}\sum_{n=1}^{N} w(\nu_n)|\alpha(\nu_n)\lambda - R(\nu_n; \xi_1, ..., \xi_P)|^2 \qquad (4)$$

where N denotes the number of frequencies of measurement per spectrum and P the number of adjustable parameters ξ_P of R. The $w(\nu_n)$ are weighing factors that have been chosen inversely proportional to the experimental errors $\Delta\alpha(\nu_n)$. To get reliable estimates of the errors in the parameters ξ_p, $p = 1$, ..., P, additional fitting procedure have been run in which sets

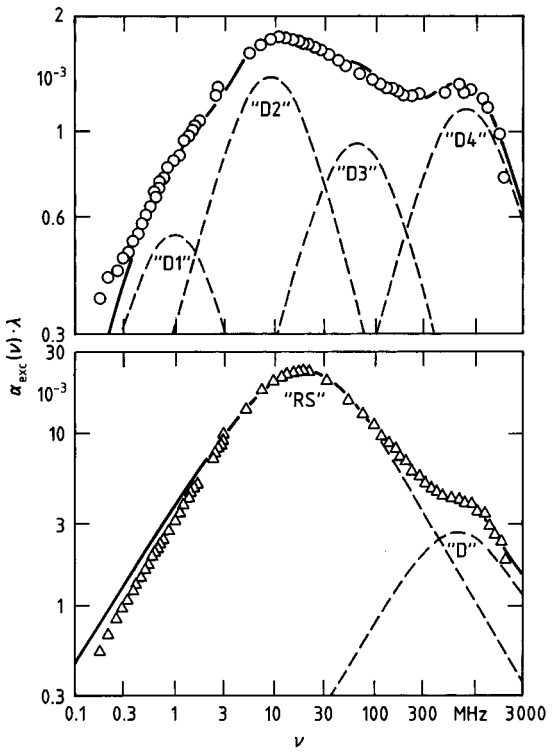

Figure 5. Ultrasonic excess absorption versus frequency ν for the 0.45 molar (○) and the 0.8 molar (△) aqueous solution of C_7ACl at 25 °C. The dashed curves indicate the subdivision of the spectra into four Debye terms ("D1" ... "D4") as well as a Romanov−Solov'ev ("RS") and a Debye ("D") term. The full curves represent the sum of these terms, respectively.

of pseudodata $\tilde{\alpha}(\nu_n)\lambda$ were treated. These pseudodata have been obtained by adding, within the limits of experimental errors $\Delta\alpha(\nu_n)$, random values to the measured values of the absorption coefficient

$$\tilde{\alpha}(\nu_n) = \alpha(\nu_n)(1 + r_n\Delta\alpha(\nu_n)/\alpha(\nu_n)) \tag{5}$$

where $r_n \in [-1,1]$, $n = 1, ..., N$.

Description of Measured Spectra by Relaxation Functions. It is an obvious attempt to represent the excess absorption spectra of the aqueous C_7ACl solutions by two Debye terms ("D",[26]) with discrete relaxation times τ_{D1} and τ_{D2}, respectively. It turned out, however, that even a sum of four Debye terms cannot adequately account for the measured excess absorption. This remarkable result is illustrated by Figure 5, where the spectrum of the 0.45 M solution is shown along with the graph of the model relaxation function

$$R_{D,D,D,D}(\nu) = \sum_{l=1}^{4} R_{Dl}(\nu) + \alpha_{cl}(\nu)$$

$$= \sum_{l=1}^{4} \frac{A_{Dl}\omega\tau_{Dl}}{1 + \omega^2\tau_{Dl}^2} + B\nu \tag{6}$$

with $\omega = 2\pi\nu$. We also tried to use functions representing continuous relaxation time distributions that are based on theoretical models. Among these functions has been the sum of a Romanov−Solov'ev term[11,12] and a Debye term

$$R_{RS,D}(\nu) = R_{RS}(\nu) + R_D(\nu) + B\nu \tag{7}$$

the sum of an extended Romanov−Solov'ev term[27] and a Debye relaxation term

$$R_{RS^*,D}(\nu) = R_{RS^*}(\nu) + R_D(\nu) + B\nu \tag{8}$$

and also a sum of a term that represents thermal and viscous boundary effects[28−30] and a Debye term

$$R_{sc,D}(\nu) = R_{sc}(\nu) + R_D(\nu) + B\nu \tag{9}$$

None of these models can represent the sets of measured absorption spectra within the limits of experimental error. As an example the discrepancy between the $R_{RS,D}(\nu)$ function and the measured $\alpha\lambda$-spectrum for the 0.8 M solution is also shown in Figure 5. A satisfactory description of the absorption data for the C_7ACl solutions, however, is enabled by a combination of the semiempirical Hill function[31,32] and a Debye term

$$R_{H,D}(\nu) = R_H(\nu) + R_D(\nu) + \alpha_{cl}(\nu)$$

$$= \frac{A_H(\omega\tau_H)^{m_H}}{(1 + (\omega\tau_H)^{2s_H})^{(m_H+n_H)/(2s_H)}} + \frac{A_D\omega\tau_D}{1 + \omega^2\tau_D^2} + B\nu \tag{10}$$

Here, m_H, n_H, and $s_H \in (0,1)$ are parameters that control the width and the shape of the underlying relaxation time distribution function. At $m_H = n_H = s_H = 1$ $R_H(\nu)$ agrees with a Debye relaxation term $R_D(\nu)$. In contrast to the nine-parameter function $R_{D,D,D,D}(\nu)$ that had been found to be less appropriate here, $R_{H,D}(\nu)$ contains eight adjustable parameters only. To further reduce the number of unknown parameters, we tried to fix one or two relaxation time distribution parameters at 1 in the fitting procedures. It was found that only with the 0.45 M and the 0.5 M solution all distribution parameters need to be different from 1 (Table 2). The parameter values for the Hill term in eq 10 as found by the regression analysis are collected in Table 2. Also given are the relaxation time $\tau_{max} = (2\pi\nu_{max})^{-1}$ and amplitude A_{max}, which correspond to the maximum in $R_H(\nu)$:

$$A_{max} = 2R_H(\nu_{max}) \tag{11}$$

$$dR_H(\nu)/d\nu|_{\nu_{max}} = 0, \quad d^2R_H(\nu)/d\nu^2|_{\nu_{max}} < 0 \tag{12}$$

These quantities have been derived from the Hill parameters using the relations

$$A_{max} = 2A_H[(m_H/n_H)^{m_H}(1 + m_H/n_H)^{-(m_H+n_H)}]^{1/(2s_H)} \tag{13}$$

and

$$\tau_{max} = \tau_H(m_H/n_H)^{-1/(2s_H)} \tag{14}$$

The values for the parameters of the Debye term and also the B-values of the C_7ACl solutions are presented along with some further data in Table 3.

4. Discussion

Relaxation in the Megahertz Frequency Region. In Figure 6 the relaxation time distribution function $G_H(\tau/\tau_H)$ corresponding to the Hill term $R_H(\nu)$ is displayed for aqueous solutions of C_7ACl. The G_H functions have been calculated from the parameters in Table 2 by analytic continuation.[33,34] As illustrated by Figure 6, at concentrations between 0.4 and 0.5 mol/L there exists a rather broad distribution of relaxation times. Hence close to the critical micelle concentration the deviations in the form of the spectrum from the predictions of theoretical models of micelle kinetics are particularly pronounced. At $c \geq 0.6$ mol/L the relaxation time distribution is smaller, indicating fair agreement with the theoretical predictions. It is only briefly

TABLE 2: Parameters of the Hill Term in the Relaxation Spectral Function Defined by Eq 10 for the Aqueous Solutions of C_7ACl at 25 °C

c, mol/L, ±0.1%	A_H, 10^{-3}, ±10%	A_{max}, 10^{-3}, ±10%	τ_H, ns, ±5%	τ_{max}, ns, ±5%	m_H, ±10%	n_H, ±10%	s_H, ±10%
0.40	1.8	0.94	2.2	2.2	1[a]	1[a]	0.5
0.45	2.2	3.5	23	14	0.5	0.2	0.9
0.50	10	12	41	28	0.9	0.5	0.9
0.60	28	33	25	19	1[a]	0.6	1[a]
0.80	45	46	11	9.4	1[a]	0.7	0.9
1.00	47	48	7.4	6.2	1[a]	0.7	0.9

[a] Parameter value has been fixed in the final run of the regression analysis.

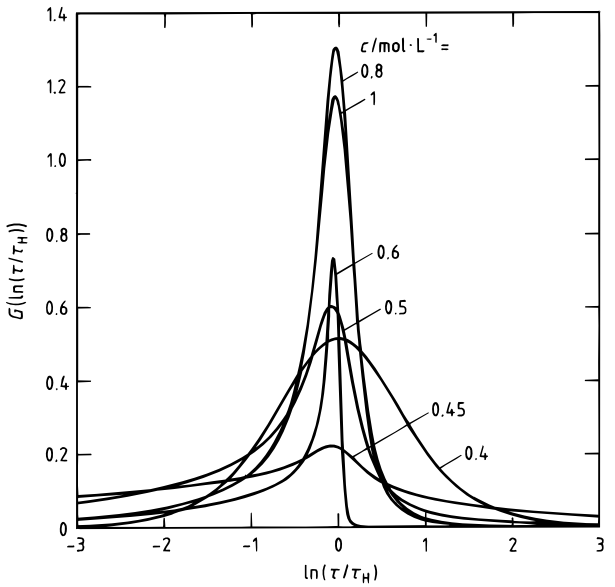

Figure 6. Relaxation time distribution function $G(\ln(\tau/\tau_H))$ displayed for the Hill term in the ultrasonic absorption spectra of the C_7ACl solutions. G has been calculated according to the relation $G(r) = (2\hat{G}/\pi)\,\mathrm{Re}\{(-ie^{-r})^m/[(1 + (-ie^{-r})2s)^{(m+n)/2s}]\}$ by analytical continuation of the Hill spectral function.[33,34] Here $r = \ln(\tau/\tau_H)$ and G is found by the normalization $\int_{\tau=0}^{\infty} G(r)\,dr = 1$.

TABLE 3: Parameters of the Debye Term and *B*-Parameter of the Relaxation Spectral Function Defined by Eq 10 as Well as the Volume Fraction Ratio v_c/v_η (Eqs 27, 35) for the Aqueous Solutions of C_7ACl at 25 °C

c, mol/L, ±0.1%	A_D, 10^{-3}, ±20%	τ_D, ns, ±50%	v_c/v_η, ±10%
0.40	1.5	0.16	
0.45	3.1	0.08	0.58
0.50	3.7	0.09	0.75
0.60	3.8	0.09	0.59
0.80	5.4	0.10	0.52
1.00	8.0	0.09	0.41

mentioned here that similar deviations of the spectrum from Debye-type relaxation behavior have been reported[45] for solutions of other short-chain amphiphiles. The relaxation amplitudes A_{max} and relaxation rates $1/\tau_{max}$ are shown as a function of concentration of amphiphile in Figure 7. Again toward higher c the behavior as predicted by the Teubner−Kahlweit theory[7,8] is approached. The amplitude and relaxation rate $c > 0.5$ mol/L nearly follow the relations

$$A_{max} = \frac{\pi(\Delta V)^2}{\kappa_s^\infty RT}\bar{N}_1 X\left(1 + \frac{\sigma^2}{\bar{m}}X\right)^{-1} \qquad (15)$$

and

$$\tau_{max}^{-1} = k^b\left(\frac{1}{\sigma^2} + \frac{X}{\bar{m}}\right) \qquad (16)$$

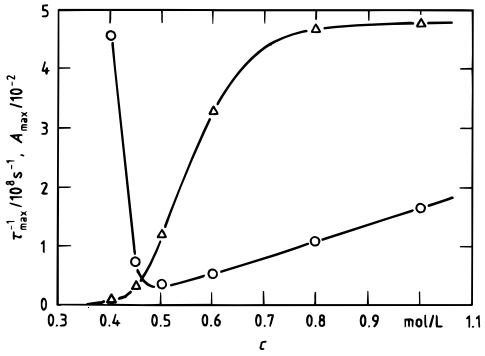

Figure 7. Relaxation amplitude A_{max} and relaxation rate τ_{max}^{-1} of the Hill term plotted versus amphiphile concentration c for the aqueous solutions of C_7ACl at 25 °C.

respectively. Here is ΔV (=ΔV_i) the reaction volume, which within the framework of the Teubner−Kahlweit theory is assumed to be the same in all steps of the scheme defined by eq 1. Effects from a more realistic choice of ΔV_i values are mentioned when discussing an extended version of the model of stepwise association.[38] k^b is the mean rate constant for the backward reactions at $i \approx \bar{m}$ (Figure 1). In deriving eqs 15 and 16 it had been assumed that

$$k_{i+1}^b \bar{N}_{i+1}/\bar{N}_i - k_i^b = (k^b/\sigma^2)(i - \bar{m}) \qquad (17)$$

corresponding with a Gaussian distribution of micelle sizes with variance σ^2. The $\bar{N}_i$ denote molar concentrations in thermal equilibrium of the system. In relation 15 κ_s^∞ is the adiabatic compressibility extrapolated to high frequencies and R is the gas constant. The dependence upon concentration of the relaxation amplitude and relaxation rate is governed by parameter X in eqs 15 and 16, respectively. X denotes the ratio of the concentrations of associated and monomer molecules of amphiphile. For long chain surfactant systems it is assumed that at $c >$ cmc the monomer concentration equals the cmc. Hence

$$X = (c - \mathrm{cmc})/\mathrm{cmc} \qquad (18)$$

As expected from eqs 15 and 16, the experimental A_{max} data reveal a saturation effect at high amphiphile concentration, and at $c > 0.5$ mol/L the τ_{max}^{-1} values in fact increase proportional to c. At $c < 0.5$ mol/L, however, the A_{max} data do not follow the concentration dependence of eq 15, and, in addition, τ_{max}^{-1} increases substantially when approaching the cmc. This latter finding seems to be characteristic of amphiphiles with small hydrocarbon chain length[14,46] and, therefore, high and less defined cmc. A similar deviation of the relaxation rate (at a concentration slightly below the cmc) has been already found by Frindi et al.[47,48] and has been attributed to the formation of aggregates with very low aggregation numbers. Obviously, the existing theories of micelle kinetics, except for the broadening of the relaxation term, apply well at concentrations distinctly

TABLE 4: Parameter Values for Three Micelle Systems with High Critical Micelle Concentration cmc, *n*-Heptylammonium Chloride (C_7ACl), Sodium Hexyl Sulfate (NaC_6S), and Sodium Heptyl Sulfate (NaC_7S) in Water at 25 °C: The Mean Aggregation Number $\bar{m}$ and Variance σ^2 of the Size Distribution of Micelles as Well as the Forward (k^f) and Backward (k^b) Rate Constants[a]

amphiphile	cmc, mol/L	$\bar{m}$	σ^2	k^f, 10^9 $(s\cdot mol/L)^{-1}$	k^b, 10^9 s^{-1}
C_7ACl	0.4	20	152	3.2	1.3
NaC_6S	0.42	17	36	3.2	1.3
NaC_7S	0.22	22	100	3.3	0.73

[a] NaC_6S and NaC_7S data have been taken from ref 14.

above the critical micelle concentration region but do not adequately represent the more complex behavior in the cmc range. For the above reasons we tentatively discuss the A_{max} and τ_{max} data at $c > 0.5$ mol/L in light of eqs 15 and 16. The reaction volume ΔV follows from the asymptotic value $A_{max,\infty} = A_{max}(c \gg \text{cmc})$ of eq 15:

$$A_{max,\infty} = \pi(\Delta V)^2 \text{cmc}/(\kappa_s^\infty RT) \tag{19}$$

Evaluating this equation the well-known relation

$$\kappa_s = \rho^{-1} c_s^{-2} \tag{20}$$

between the isentropic compressibility κ_s and the sound velocity c_s is utilized to estimate κ_s at frequencies well above the relaxation regions. In the numerical calculations c_s data at 520 MHz (Table 1) are simply used here and $\kappa_s^\infty = 4.1 \times 10^{-10}$ Pa^{-1} as well as $\Delta V = 6.2$ cm^3 mol^{-1} are found as reasonable estimates. The latter value agrees nicely with the reaction volume for sodium heptyl sulfate, NaC_7S.[7] With the value for ΔV the ratio $\sigma^2/\bar{m}$ can be obtained from a fit of eq 15 to the measured A_{max} data. Assuming $\bar{m} = 20$ the velocity constant k^b according to eq 16 can be derived from the experimental τ_{max} values. Finally, we use the relation

$$k_i^f = k_i^b \bar{N}_i / (\bar{N}_1 \bar{N}_{i-1}) \tag{21}$$

at $i \approx \bar{m}$, where $\bar{N}_{i-1} \approx \bar{N}_i$ and thus

$$k^f \approx k^b/\text{cmc} \tag{22}$$

to calculate k^f. According to the law of action of mass, eq 21 follows directly from the reaction scheme defined by eq 1. The k^f, k^b, and σ^2 values resulting from this estimation of data are listed in Table 4 where, for comparison, the corresponding data for solutions of sodium hexyl sulfate (NaC_6S) and NaC_7S are also presented.[14] The rate constants for the aqueous C_7ACl solutions agree nicely with those for solutions of NaC_6S, a surfactant of similar cmc (Table 4). It is also interesting to notice that the k^f values of the three amphiphile solutions point at a diffusion-controlled incorporation of monomers in the micellar structures.

Debye-type Relaxation around 1 GHz. In previous ultrasonic relaxation studies of aqueous solutions of amphiphiles,[9,10] the Debye term with small relaxation time τ_D around 10^{-10} s has been attributed to mechanisms of rotational isomerization of the hydrocarbon chains in the micellar core. Hence the Debye-type relaxation has been assumed to reflect a chemical equilibrium

$$C \underset{k^b_C}{\overset{k^f_C}{\rightleftharpoons}} C^* \tag{23}$$

with relaxation rate[6]

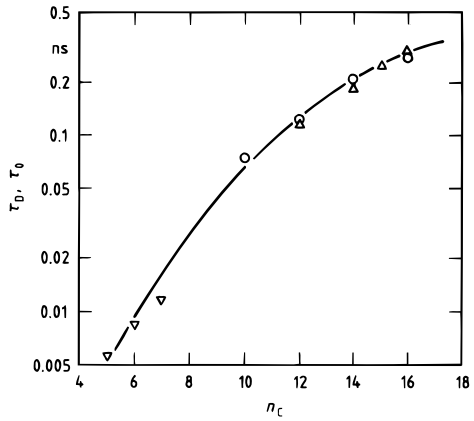

Figure 8. Ultrasonic relaxation time τ_D at 25 °C (○, ref 35) as well as structure relaxation time τ_0 derived from depolarized light scattering at 21 °C (▽, ref 36) and 25 °C (△ ref 37) displayed as a function of the number n_C of carbon atoms for some normal alkanes CH_3-$(CH_2)_{n_C-2}CH_3$.

$$\tau_D^{-1} = k_C^f + k_C^b \tag{24}$$

indepent of concentration. If the τ_D-value for the solution with lowest concentration $c = 0.4$ mol/L (≈cmc) is left out of consideration here, then in fact a constant relaxation rate $\bar{\tau}_D^{-1}$ follows from our measurements (Table 3). The mean relaxation time $\bar{\tau}_D$ for the C_7ACl solutions, however, does not fit to the expectations based on relaxation times for pure *n*-alkanes. In Figure 8 ultrasonic relaxation times τ_D[35] and also structure relaxation times τ_0 from depolarized light-scattering measurements[36,37] of alkanes are displayed as a function of the number n_C of hydrocarbon groups per molecules. The $\bar{\tau}_D$ value for the present micelle system is nearly 1 order of magnitude higher than predicted by the relaxation time-versus-n_C relation for alkanes. This discrepancy might—at least in part—be due to an oversimplification of the solution properties here, neglecting any effects of surface tension and assuming the same molecular order, dynamics, and microviscosity to exist in the micellar core of short-chain amphiphiles as in liquid alkanes. It may, however, be also a reflection of another relaxation mechanism that additionally contributes to the Debye term as will be detailed discussed in the second part of this study.[38] The amplitude A_D of the spectral term that is related to the unimolecular reaction eq 23 is given by the relation[39]

$$A_D = \pi d\kappa_s/\kappa_s^0 \tag{25}$$

where κ_s^0 denotes the adiabatic compressibility extrapolated to low frequencies and $d\kappa_s$ the compressibility change accompanied with the elementary chemical process. To look for the relevance of the supposed structural isomerization effect in the A_D values, let us assume the simple mixture relation[40]

$$\kappa_s^0 = v_c \kappa_{sc}^0 + (1 - v_c)\kappa_{sv}^0 \tag{26}$$

to represent the compressibility of the heterogeneous micelle solutions appropriately. Herein v_c denotes the volume fraction of the micellar core and κ_{sc}^0 and κ_{sv}^0 are the isentropic compressibilities of the core and the solvent, respectively. Using eq 26 the headgroup region of the micelles together with the suspending phase is simply treated as a homogeneous solvent. Let ϕ_{C7} denote the molar volume of a heptyl chain. The volume fraction of the micelle cores is then given by the equation

$$v_c = (c - \text{cmc})\, \phi_{C7} \tag{27}$$

If eqs 25−27 are combined, the concentration dependence of the relaxation amplitude can be written as

$$A_D^{-1} = \frac{\kappa_{sv}^0}{\pi d \kappa_s}[1 + (c - \mathrm{cmc})\phi_{C7}(\kappa_{sc}^0/\kappa_{sv}^0 - 1)] \quad (28)$$

From this equation follows

$$\frac{\kappa_{sc}^0}{\kappa_{sv}^0} = \phi_{C7}^{-1} \frac{1}{A_D^{-1}(\mathrm{cmc})} \frac{dA_D^{-1}(c)}{dc} + 1 \quad (29)$$

where

$$A_D^{-1}(\mathrm{cmc}) = \kappa_{sv}^0/(\pi d \kappa_s) \quad (30)$$

With the A_D data given in Table 3 and with $\phi_{C7} = 70$ mL/mol taken from the density of *n*-heptane, the ratio $\kappa_{sc}^0/\kappa_{sv}^0 = 12 \pm 4$ results. This value appears to be too high, and it may thus be considered another indication of the Debye-type relaxation term in the C_7ACl/water spectra to be not solely due to rotational isomerizations in the micellar core.

Classical Absorption and Volume Viscosity. According to ultrasonic scattering theory,[30] the *B*-parameters of the micelle solutions according to

$$B = B_v + \frac{c_{sv}\nu_m}{2}\left[B_v\left(\frac{\rho_v c_{sv}}{\rho_m c_{sm}^2} - \frac{3}{c_{sv}}\right) + 2B_m \frac{\rho_v}{\rho_m c_{sm}}\right] \quad (31)$$

are related to the *B*-values, densities ρ, and sound velocities of the micelles ("m") and of the suspending solvent ("v"). In eq 31 ν_m denotes the volume fraction of micelles. Equation 31 may be written as

$$B - B_v = \nu_m \frac{\rho_v c_{sv}}{\rho_m c_{sm}}\left[\frac{1}{2}B_v\left(\frac{c_{sv}}{c_{sm}} - 3\frac{\rho_m c_{sm}}{\rho_v c_{sv}}\right) + B_m\right] \quad (32)$$

The *B*-values of the micelle solutions are found to be nearly independent of solute concentration and thus of the volume fraction of the micelles (Table 3). Hence with the reasonable assumption that $dB_v/d\nu_m \approx 0$ at $c >$ cmc

$$B_m \approx \left[3\frac{\rho_m c_{sm}}{\rho_v c_{sv}} - \frac{c_{sv}}{c_{sm}}\right]\frac{B_v}{2} \quad (33)$$

follows for the present micelle solutions. Unfortunately, we do not know the correct density and sound velocity values to be used in eq 33. Let us, therefore, assume the solvent data to nearly agree with those for solutions at the cmc (≈0.4 mol/L) and let us insert *n*-heptane data as a rough estimate for ρ_m and c_{sm}. If this is accepted, $B_m \approx 0.15 B_v$ results. This B_m value appears to be too small as compared to $B_m \approx 40 \times 10^{-12}$ s $> B_v(\mathrm{cmc}) = 33 \times 10^{-12}$ s that follows from extrapolation of the *B*-data of a series of normal alkanes from *n*-decane to *n*-hexadecane.[35] Hence we conclude that the above assumptions are not fulfilled here. Particularly $dB_v/d\nu_m \approx 0$ may be questioned. According to the generally accepted relation[41]

$$B_v = B_{vs} + B_{vv} = \frac{2\pi^2}{c_{sv}^2 \rho_v}\left(\frac{4}{3}\eta_{sv} + \eta_{vv}\right) \quad (34)$$

the classical absorption of the solvent is composed of two parts; one is given by the shear viscosity η_{sv} and the other one by the so-called volume viscosity[41] η_{vv} of the solvent. For water with its voluminous hydrogen-bonded structure and a suggested structural relaxation well above our frequency range of measurements, the high volume viscosity $\eta_v = 2.68\eta_s$ results at 25 °C.[42] It is frequently found that the η_v/η_s ratio substantially decreases when solutes are added to water (e.g. ref 27). In many cases even the limiting value $\eta_v = 0.67\eta_s$ is adopted at enhanced solute concentration. This value has been predicted for liquids without high-frequency structural relaxation.[43,44] Constancy of the *B*-data (Table 3) thus seems to reflect the compensation of the contribution from the micelles that increases with ν_m by the B_v contribution. The latter decreases significantly with ν_m, not only due to the decreasing volume fraction of solvent but also as a result of a reduction of the η_{vv} part in B_v.

Shear Viscosity and Volume Fraction of Micelles. Following Einstein, the shear viscosity ratio η_s/η_{sv} is related to the hydrodynamic volume fraction ν_η of micelles according to[13]

$$\eta_s/\eta_{sv} = 1 + 2.5\nu_\eta \quad (35)$$

If $\eta_{sv} = \eta_s$ (0.4 mol/L) is used as the solvent shear viscosity in this equation, the ν_η data listed in Table 3 result. Also presented in Table 3 is the volume fraction ratio ν_c/ν_η where ν_c again denotes the volume fraction of the micellar cores as defined by eq 27. In conformity with our expectations $\nu_c/\nu_\eta < 1$ is found throughout since ν_η in addition to ν_c contains contribution from the headgroup region of the micelles. The ν_c/ν_η values decreases when going from the 0.5 molar solution to mixtures of higher micelle content. This finding obviously indicates interactions between micelles at high solute concentration that are not considered by the Einstein relation eq 35. The fact that ν_c/ν_η is substantially smaller at $c = 0.45$ mol/L than at $c = 0.5$ mol/L, however, is another indication for geometrically less defined supramolecular (oligomeric) structures to exist at concentrations in the cmc range rather than globular micelles.

Acknowledgment. We thank Professor R. Pottel and Dr. K. Lautscham for valuable discussions. Financial support by the Deutsche Forschungsgemeinschaft is gratefully acknowledged.

References and Notes

(1) Mittal, K. L., Lindman, B., Eds. *Surfactants in Solution*; Plenum: New York, 1984.
(2) Degiorgio, V., Corti, M., Eds. *Physics of Amphiphiles: Micelles, Vesicles and Microemulsions*; North-Holland: Amsterdam, 1985.
(3) Degiorgio, V. *Europhys. News* **1985**, *16*, 9.
(4) Aniansson, E. A. G.; Wall, S. N. *J. Phys. Chem.* **1974**, *78*, 1024.
(5) Aniansson, E. A. G. Prog. *Colloid Polym. Sci.* **1985**, *70*, 2.
(6) Strehlow, H.; Knoche, W. *Fundamentals of Chemical Relaxation*; Verlag Chemie: Weinheim, 1977.
(7) Teubner, M. *J. Phys. Chem.* **1979**, *83*, 2917.
(8) Kahlweit, M.; Teubner, M. *Adv. Colloid Interface Sci.* **1980**, *13*, 1.
(9) Kaatze, U.; Lautscham, K.; Berger, W. *Z. Phys. Chem. (München)* **1988**, *159*, 161.
(10) Kaatze, U.; Berger, W.; Lautscham, K. *Ber. Bunsen-Ges. Phys. Chem.* **1988**, *92*, 872.
(11) Romanov, V. P.; Solov'ev, V. A. *Sov. Phys. Acoust.* **1965**, *11*, 68.
(12) Romanov, V. P.; Solov'ev, V. A. *Sov. Phys. Acoust.* **1965**, *11*, 219.
(13) Zana, R. *Surfactant Solutions, New Methods of Investigations*; Dekker: New York, 1987.
(14) Hall, D. G.; Wyn-Jones, E. *J. Mol. Liq.* **1986**, *32*, 63.
(15) Kaatze, U.; Limberg, C. H.; Pottel, R. *Ber. Bunsen-Ges. Phys. Chem.* **1974**, *78*, 555.
(16) Kaatze, U.; Limberg, C. H.; Pottel, R. *Ber. Bunsen-Ges. Phys. Chem.* **1974**, *78*. 561.
(17) Edmonds, P. D. *Ultrasonics*; Academic: New York, 1981.
(18) Kaatze, U.; Wehrmann, B.; Pottel, R. *J. Phys. E: Sci. Instrum.* **1987**, *20*, 1025.
(19) Eggers, F; Kaatze, U. *Meas. Sci. Technol.* **1996**, *7*, 1.
(20) Eggers, F.; Kaatze, U.; Richmann, K. H.; Telgmann, T. *Meas. Sci. Technol.* **1994**, *5*, 1131.
(21) Kaatze, U.; Lautscham, K. *J. Phys. E: Sci. Instrum.* **1986**, *21*, 402.
(22) Kaatze, U.; Kühnel, V.; Menzel, K.; Schwerdtfeger, S. *Meas. Sci. Technol.* **1993**, *4*, 1257.

(23) Kaatze, U.; Lautscham, K.; Brai, M. *J. Phys. E: Sci. Instrum.* **1988**, *21*, 98.
(24) Kaatze, U.; Kühnel, V.; Weiss, G. *Ultrasonics* **1996**, *34*, 51.
(25) Bömmel, H. E.; Dransfeld, K. *Phys. Rev. Lett.* **1958**, *1*, 234.
(26) Debye, P. *Polare Molekeln*; Hirzel: Leipzig, 1929.
(27) Kühnel, V.; Kaatze, U. *J. Phys. Chem.*, in press.
(28) Epstein, P. S.; Carhart, R. R. *J. Acoust. Soc. Am.* **1953**, *25*, 553.
(29) Allegra, J. R.; Hawley, S. A. *J. Acoust. Soc. Am.* **1972**, *51*, 1545.
(30) Kaatze, U.; Trachimow, C; Pottel, R.; Brai, M. *Ann. Phys.* **1996**, *5*, 13.
(31) Hill; R. M. *Nature* **1978**, *275*, 96.
(32) Hill, R. M. *Phys. Status Solidi* **1981**, *103*, 319.
(33) Giese, K. *Adv. Mol. Relax. Processes* **1973**, *5*, 363.
(34) Menzel, K. Dissertation; Georg-August-University; Göttingen, 1993.
(35) Kaatze, U.; Lautscham, K.; Berger, W. *Chem. Phys. Lett.* **1988**, *144*, 273.
(36) Volterra, V.; Bucaro, J. A.; Litovitz, T. A. *Ber. Bunsen-Ges. Phys. Chem.* **1971**, *75*, 309.
(37) Champion, J. V.; Jackson, D. A. In *Molecular Motions in Liquids*; Lascombe, J., Ed.; Reidel: Dordrecht, 1974; p 585.
(38) Telgmann, T.; Kaatze, U. *J. Phys. Chem. B* **1997**, *101*, 7766.
(39) Matheson, A. J. *Molecular Acoustics*; Wiley: London, 1971.
(40) Morse, P. M.; Ingard, K. U. *Theoretical Acoustics*; McGraw-Hill: New York, 1968.
(41) Davis, C. M.; Jarzynski, J. In *Water, a Comprehensive Treatise*; Franks, F., Ed.; Plenum: New York, 1972; Vol. 1, p 443.
(42) Litovitz, T. A.; Davis, C. M In *Physical Acoustics*; Mason, W. P., Ed.; Academic: New York, 1965; Vol. 2A; p 282.
(43) Madigoski, W. M.; Warfield, R. W. *J. Chem. Phys.* **1983**, *78*, 1912.
(44) Madigoski, W. M.; Warfield, R. W. *Acustica* **1984**, *55*, 123.
(45) Rassing, J.; Wyn-Jones, E. *Chem. Phys. Lett.* **1973**, *21*, 93.
(46) Kato, S.; Nomura, H.; Honda, H.; Zielinsky, R.; Ikeda, S. *J. Phys. Chem.* **1988**, *92*, 2305.
(47) Frindi, M.; Michels, B.; Zana, R. *J. Phys. Chem.* **1994**, *98*, 6607.
(48) Frindi, M.; Michels, B.; Levy, H.; Zana, R. *Langmuir* **1994**, *10*, 1140.